Applied Physics A (2021) 127:244
https://doi.org/10.1007/s00339-021-04391-2

Applied Physics A
Materials Science & Processing

High-sensitivity Hg^{2+} sensor based on the optical properties of silver nanoparticles synthesized with aqueous leaf extract of *Mimusops coriacea*

Carla Regina Borges Lopes[1] · Dário Santos Junior[2] · Flávia Rodrigues de Oliveira Silva[3] · Lilia Coronato Courrol[1]

Received: 24 October 2020 / Accepted: 24 February 2021 / Published online: 12 March 2021
© The Author(s), under exclusive licence to Springer-Verlag GmbH, DE part of Springer Nature 2021

Abstract

In the presented manuscript, spherical silver nanoparticles (AgNPs) which were prepared via green chemical method in a single step take only a few minutes to be ready as a Hg^{2+} ions detector based on the plasmon band changes. The AgNPs were obtained with the aqueous extract of *Mimusops coriacea* leaves. The components of the extract as tannins and polyphenolic compounds were responsible for the reduction in metal ions and the particles encapsulation. The AgNPs were characterized by UV–Vis spectroscopy, fluorescence, Fourier transform infrared, dynamic light scattering analysis and transmission electron microscopy. The AgNps presented an average diameter of 15 nm and a zeta potential value of ~ − 28 mV. They were monodispersed and stable for up to 180 days. AgNPs are used as a Hg^{2+} sensor with high sensitivity and selectivity. The fast, simple and low-cost method is based on changes in the AgNP surface plasmon resonance band ($\lambda \approx 410$ nm) with LOD 6.5 ng/mL (32.5 nM), without functionalization of the AgNPs. The low LOD demonstrates its potential for Hg^{2+} quantification in environmental samples such as fish, soil, and effluent discharge.

✉ Carla Regina Borges Lopes
carla.regina@unifesp.br

[1] Departamento de Física, Universidade Federal de São Paulo, Diadema, SP, Brazil

[2] Departamento de Química, Universidade Federal de São Paulo, Diadema, SP, Brazil

[3] Instituto de Pesquisas Energéticas e Nucleares, São Paulo, SP, Brazil

Graphic abstract

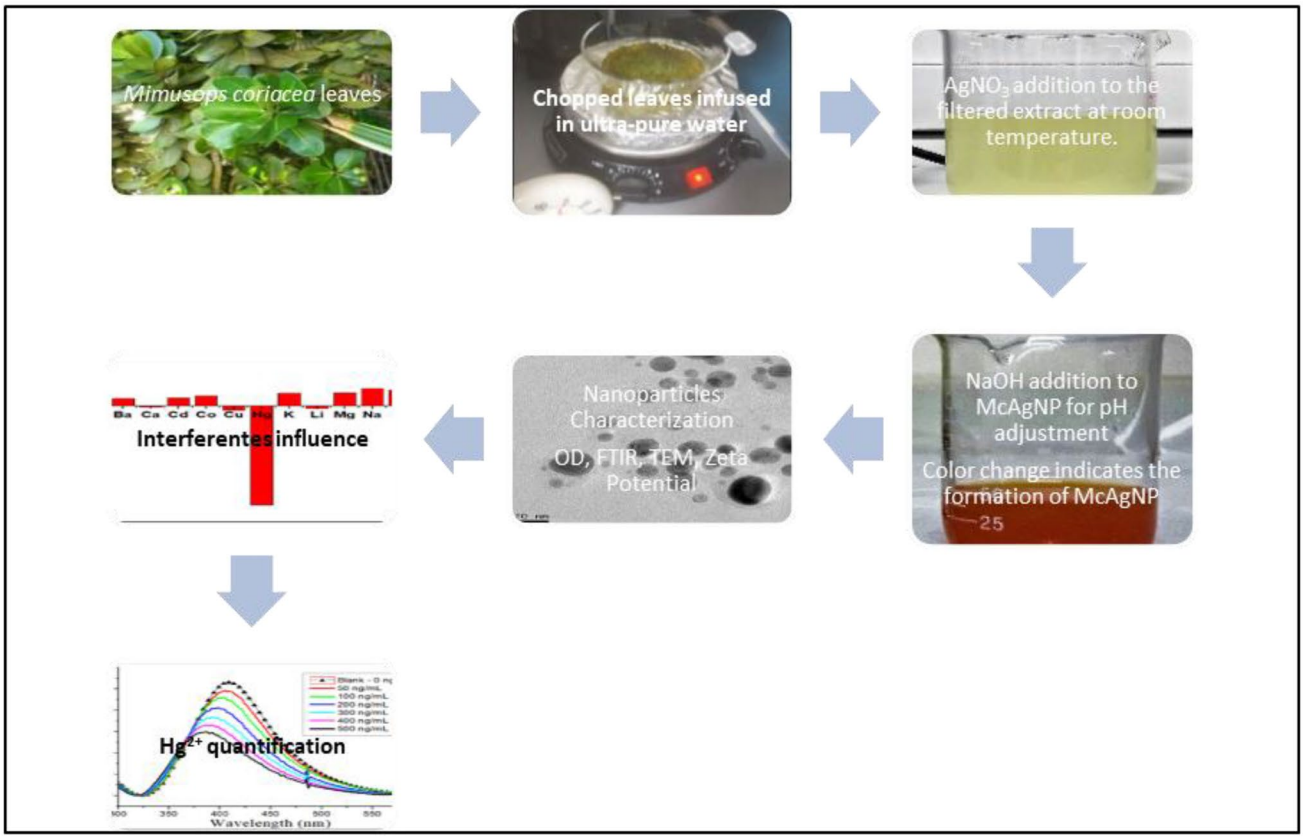

Keywords Hg sensor · Silver nanoparticles · Green synthesis · *Mimusops coriacea* · Surface plasmon resonance

1 Introduction

Mercury (Hg) is a hazardous substance, because of its ecosystems accumulation, atmospheric propagation and adverse effects on human health. Its toxicity is recognized by the International Classification of Disease [1]. It occurs in liquid state at room temperature, and increasing the temperature, it volatizes to the atmosphere, which generates colorless and odorless toxic vapors.

Methylmercury which is one of the most toxic arrangements of the metal is rapidly absorbed by aquatic organisms and thus bioaccumulated and biomagnified along the trophic chain. In this way, the living beings located at the highest trophic levels exhibit the highest concentrations of this metal. Predatory fish, such as dogfish and Tucunaré, for example, tend to have higher concentrations of Hg and may lead to contamination of the population who feeds on these species [2, 3].

Due to the high toxicity of Hg even at low concentrations, several analytical techniques for its determination have been developed in recent years. Most of them are based on chromatographic techniques [4]. Although extremely sensitive and selective, these methods depend on high-cost equipment and, in general, complex sample preparation procedures.

Metallic nanoparticles (MNP) such as silver (AgNP) and gold (AuNP) have been reported with excellent results in the development of colorimetric methods for the detection of contaminants [5–9]. However, the methods traditionally used to achieve nanoparticles (NPs) involve the use of toxic chemical reducers which limits its application in the clinical and pharmaceutical field, also the possibility of the generation of residues potentially harmful to the environment and to human health [10]. Against this backdrop, the search for safer procedures with less impact on the environment, which is denominated green synthesis, rises. These methods' purpose is to use biological systems in replacement of toxic chemical reagents in order to attain nanomaterials. These methods are a sustainable alternative, which result in high biocompatibility and biodegradability NPs by low production cost of production and high yield [11–17]

Several studies have been published in the last two decades regarding metallic nanoparticles synthesis mediated by plants. In general, the processes involve aqueous extracts from different parts of the plants and the authors indicate secondary metabolites present in these extracts as responsible for the reduction in the metal ions and for ensuring the nonaggregation of the particles [18–22].

Studies on the use of MNP in the determination of Hg^{2+} have been published in recent years. However, the synthesis of MNP and the Hg^{2+} detection depend on long, complex and strictly controlled procedures, and MNP functionalization involves the use of toxic reagents and expensive materials [23–28].

Some studies have reported Hg detection by MNP obtained by green methods. However, the synthesis process usually depends on multiple steps. Ghosh et al. [29] reported the detection of AgNPs obtained by plant extracts. The time required to obtain the plant extract and for the formation of the reported AgNP was greater than 24 h, depending on sun exposure and centrifugation process. The detection limit obtained was 2 µM.

In the present study, spherical AgNPs (diameter≅15 nm) were synthesized using the *Mimusops coriacea*'s leaves aqueous extract (McAgNP). This plant, which is African originated, produces a fruit rich in vitamins known as apricot. The McAgNPs obtained were applied in the development of a method for the detection of Hg^{2+} in aqueous solution. This method is based on the NPs change in its SPR bands with a detection limit of 32 nM.

The synthesis method has been simplified compared to the previously published one [22]. The xenon lamp irradiation step which is used in the previous procedure was eliminated, and nanoparticle synthesis was controlled by pH adjustments. In this study, the formation of AgNP occurs in a few minutes using a single-stage method, at room temperature and neutral pH. This method has shown high yield and reproducibility, even when considering the climatic changes that the plant is exposed to throughout the year. The Hg^{2+} detection method is fast and simple. It consists of mixing the sample (aqueous solution) with the nanoparticles and reading the absorbance signal ($\lambda \sim 405$ nm). It has high sensitivity, selectivity and reproducibility. Until this date, we have not found reports of an AgNP synthesis method with similar simplicity that is effective in detecting Hg^{2+} with a compatible detection limit.

2 Materials and methods

2.1 Synthesis and characterization of silver nanoparticles (McAgNP)

The employed method to obtain McAgNP was based on the one that was reported on a previous study [22], with modifications. In this work, the xenon lamp irradiation step was eliminated, and the synthesis takes place at room temperature.

The effects on the variation in the silver nitrate ($AgNO_3$) concentration, the plant material volume and the reaction pH during the colloidal suspension preparation were analyzed. These studies are detailed in Table S1 in Electronic Supplementary Information 1 (ESM 1).

In order to prepare the aqueous extract, the *M. coriacea* leaves were collected on the Prainha Branca Coast, which is located in the Serra do Guararu Environmental Preservation Area, Guarujá, São Paulo, Brazil, at latitude − 23.869296 and longitude − 46.137139.

The collected plant material was washed with distilled water and chopped into pieces of approximately 10 × 3 mm. The material was than infused for 5 min in 100 mL of ultrapure water at a mean temperature of 82 °C (± 2 °C) on a magnetic stirrer with heating (Fisatom 753A). After one minute of standing, the material was filtered on a plain filter paper. The attained yield was approximately 80 mL of extract, which consisted of a light-green liquid. The extracts were prepared within 24 h after harvesting the leaves.

The silver nanoparticle suspension (McAgNP) was prepared from the $AgNO_3$ (Sigma-Aldrich) and diluted in 40 mL of the extract at room temperature. The pH of the reaction was adjusted by adding sodium hydroxide (NaOH) in aqueous solution at a concentration of 1 mmol.

The McAgNPs were characterized by absorption spectrometry techniques in UV–Vis (Shimadzu MultiSpec 1501 spectrophotometer) and infrared regions (FTIR Shimadzu IRPrestige-21). The fluorescence spectra of synthesized samples were obtained by exciting samples in the chlorophyll

Table 1 Variations in the preparation of McAgNP

Name	M.c Leaves (mg\mL) (± 2 mg)	$AgNO_3$ (mmol/L)	Initial pH (± 0.1)	Adjusted pH #1(± 0.1)	Adjusted pH #2 (± 0.1)
McAg1	25	1	5.83	6.92	10.10
McAg2	25	2	5.90	7.45	10.21
McAg3	50	1	5.40	7.39	9.80
McAg4	50	2	5.05	6.78	10.76
McAg5	100	1	5.30	7.16	9.87
McAg6	100	2	5.32	6.99	10.54

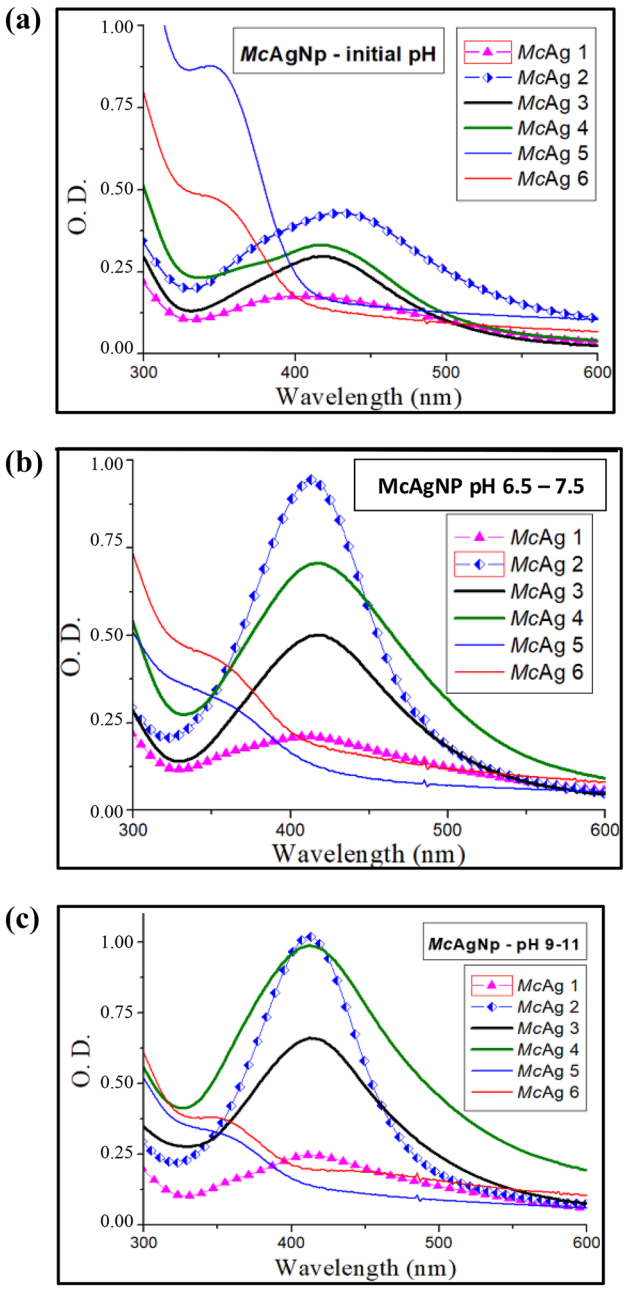

Fig. 1 UV–Vis spectra of McAgNP

Table 2 Results of McAg 2 DLS analyses (pH ~ 7.5)

Hydrodynamic diameter (nm)	Vol(%)	PDI	Zeta potential (mV)
95.89 (±59.42)	59.7		
1230 (±395.0)	6.7	0.239	−28.0 (±0.43)
27.53 (±5.45)	33.0		

absorption band, which is around 430 nm with the fluorometer Fluorolog 3 (Horiba Jobin Yvon). Transmission electron

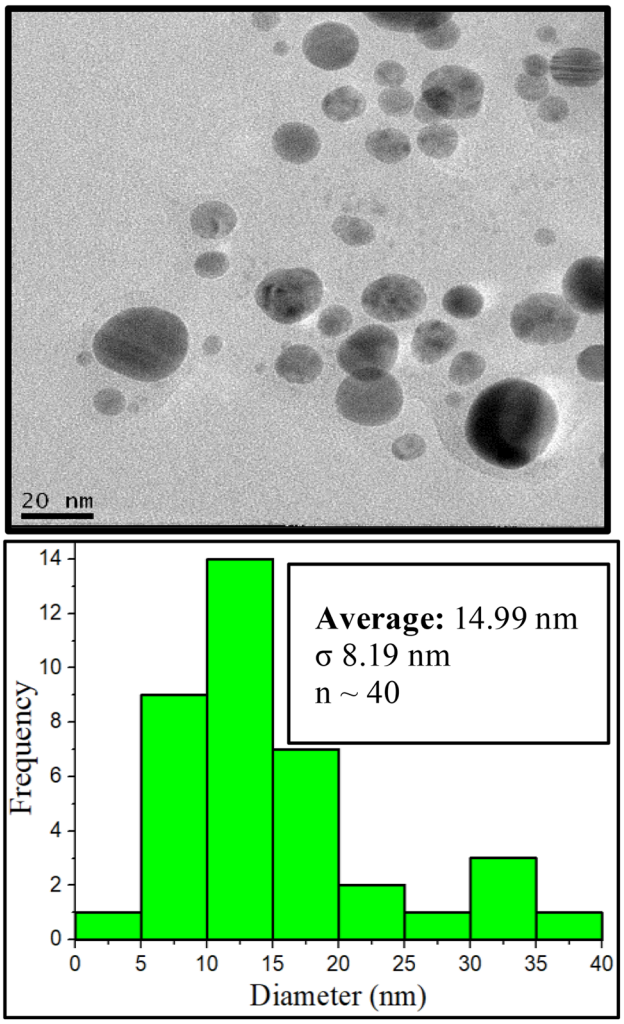

Fig. 2 TEM images and size distribution histogram of McAg 2 pH ~ 7.5

microscopy (TEM) images were obtained to determine the shape and size of the particles (JEM 2100-JEOL). The stability of colloidal suspensions was analyzed by measures of zeta potential (Zetasizer Nano ZS Malvern). The procedures used are detailed in a previous study [22].

In this work, the particle size distribution considering its hydrodynamic diameter and polydispersity was analyzed by dynamic light scattering (DLS) by Zetasizer Nano ZS Malvern. The scattering angle was set at 173°, the temperature was set to 25 °C and the sample stabilization time was set at 120 s. This analysis also provides information about the polydispersity (PDI) of the suspension: the closer it to 1, the more polydisperse is the solution, i.e., more heterogeneous.

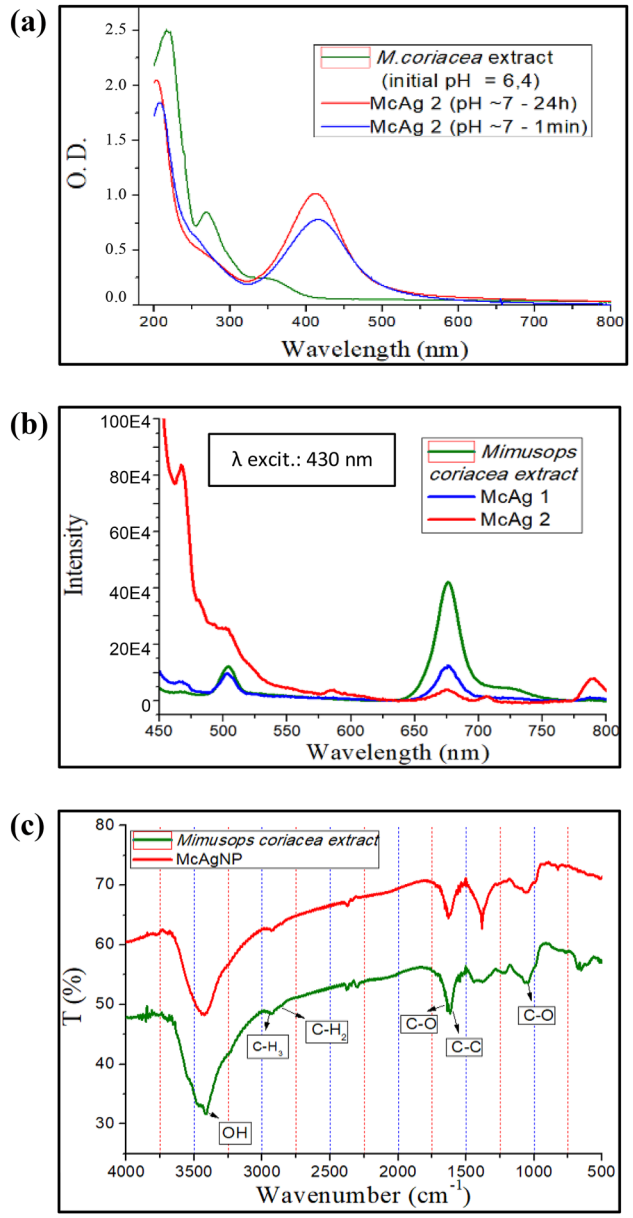

Fig. 3 UV–Vis spectrum of **a** aqueous extract of *Mimusops coriacea* 25 mg/mL and McAgNP. **b** Chlorophyll and McAgNP fluorescence spectra. **c** FTIR spectra of the *Mimusops coriacea* and McAgNP extract

2.2 Determination of Hg^{2+} in aqueous solution

2.2.1 Selectivity analysis

To determine the selectivity of the method, UV–Vis spectrophotometry measurements were performed with McAgNP in the presence of Li^{+}, Na^{+}, K^{+}, Mg^{2+}, Ca^{2+}, Sr^{2+}, Ba^{2+}, Ni^{2+}, Cu^{2+}, Zn^{2+}, Hg^{2+}, Co^{2+} e Cd^{2+} cations at a concentration of 100 µg / mL (± 3 µg/mL).

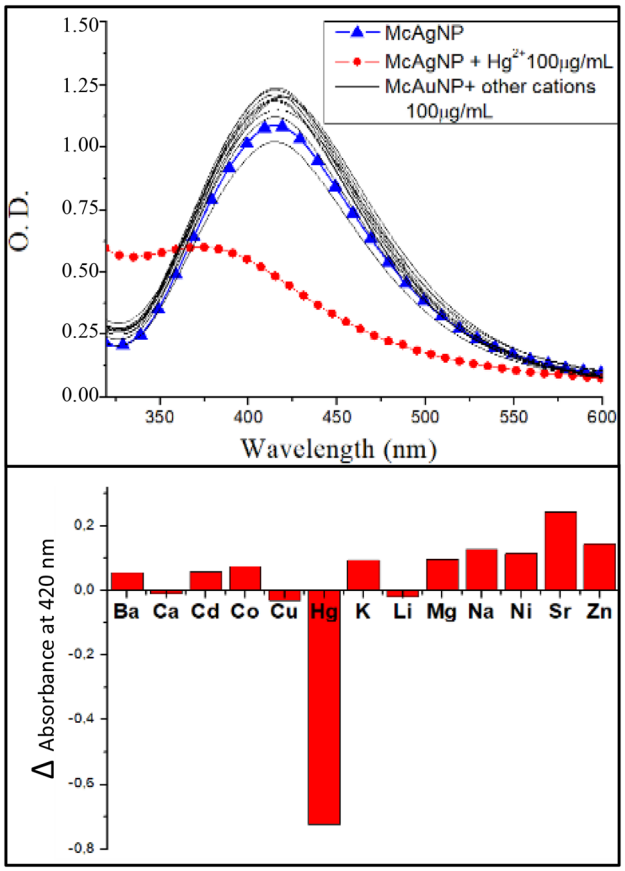

Fig. 4 Variation in the absorbance intensity of McAgNP in the presence of contaminants

2.2.2 Sensitivity of Hg^{2+} and calibration curve

A stock solution of Hg^{2+} of 100 µg/mL (± 5 µg/mL) was

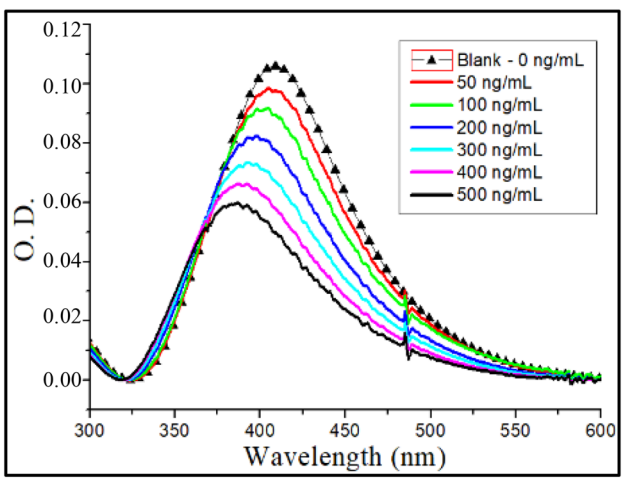

Fig. 5 UV–Vis spectra of McAgNP diluted to 10% in the presence of aqueous solutions of $Hg^{2+}$with concentrations between 50 and 500 ng/mL

(a)

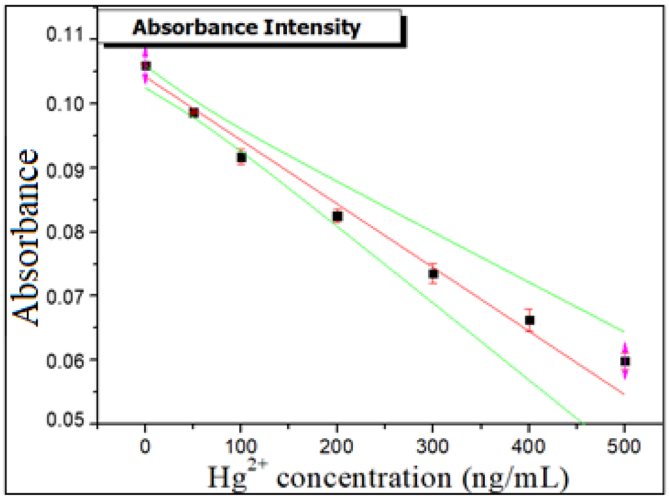

LOD= 7.87 ng / mL
LOQ= 26.26 ng / mL

Equati	y = a + b*x		
Adj. R-	0,95917		
		Value	Standard Error
	Intercept	0,10423	1,59049E-4
	Slope	-9,92632E-5	1,94305E-6

(b)

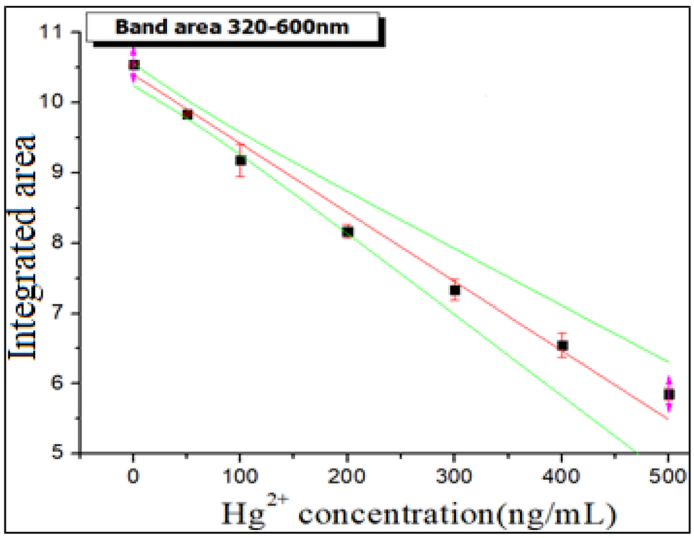

LOD= 6.52 ng / mL
LOQ=21.73 ng / mL

Equation	y = a + b*x		
Adj. R-Squ	0,97068		
		Value	Standard Error
	Intercept	10,403	0,01391
	Slope	-0,0098	1,57128E-4

(c)

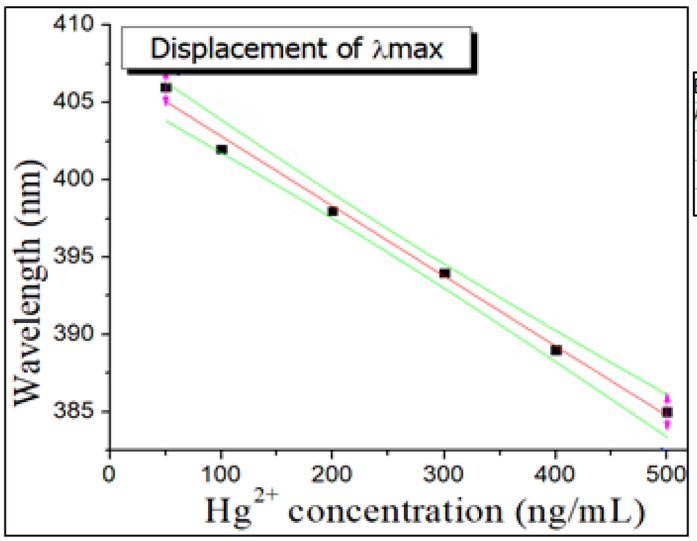

LOD= 34.66 ng / mL
LOQ=115.55 ng / mL

Equation	y = a + b*x		
Adj. R-Square	0,99285		
		Value	Standard Error
	Intercept	407,3589	0,52079
	Slope	-0,04526	0,00172

◂**Fig. 6** Analytical curves for quantification of Hg^{2+}. Green lines represent the confidence band (95%). **a** In terms of the absorbance intensity **b** Changes in the band area between 320 and 600 nm. **c** Displacement of λmax

prepared by adding 10 mL (± 0.5 mL) of a standard Hg^{2+} solution of 1000 µg/mL (± 5 µg/mL) SpecSol, in a 100-mL volumetric flask. Afterward, the flask was filled with high-purity water.

The McAgNP sensitivity analysis was performed by preparing Hg solutions with concentrations between 50 and 500 ng/mL (± 2 ng/mL). The solutions were prepared by diluting the stock solution in high-purity water.

The McAgNPs characterization has shown the best synthetic conditions. The McAgNP suspensions were diluted 1:10 in high-purity water. Furthermore, the analysis samples were prepared by mixing 1 mL of already diluted McAgNP (1:10) and 5 mL of the previous prepared Hg^{2+} solutions. So, measurements were carried out for the samples by UV–Vis spectrophotometry.

A study has been developed, in which we have varied the McAgNp, and we have analyzed the ratio between McAgNP and Hg. The measurements were carried out in triplicate, and the obtained spectra were used to fit an analytical curve and to calculate the limits of detection (LOD) and quantification (LOQ) through Eqs. 1 and 2 [30]:

$$\mathrm{LOD} = \frac{3\sigma}{b} \tag{1}$$

$$\mathrm{LOQ} = \frac{10\sigma}{b} \tag{2}$$

where LOD corresponds to the detection limit, LOQ is the limit of quantification, σ is the standard deviation of ten measurements of the analytical blank and b is the slope of the calibration curve.

3 Results

The McAgNP suspension was firstly detected because of the solution's color. The reddish-brown tone is characteristic of silver nanoparticles resulting from surface plasmon resonance (SPR), where the observed color is complementary to the absorption wavelength of the plasmon.

In the first study about the synthesis conditions, the $AgNO_3$ concentration was varied and the volume of plant material in the preparation of the extract was fixed in 50 mg/mL. It was observed that the solution color onset changes from a yellowish solution to dark-brown one after 10 min. This result was obtained with higher intensities at higher concentrations of $AgNO_3$.

UV–Vis spectrophotometry analyses showed the presence of McAgNP in suspension from the concentration of 1 mmol/L $AgNO_3$. The absorbance became more intense with increasing concentration of the metal in the solution, saturating at 2 mmol/L, since little change was observed with increasing concentration.

The absorbance intensity shift as a reaction time function was analyzed: the reaction starts immediately with significant growth up to 30 min, continuing in slower growth up to 60 min when it seems to stabilize (see Figs. S1 and S2 in ESM 1).

The *M. coriacea* leaf extract's pH is 6.5 (± 0.2). After the reaction with $AgNO_3$ and the formation of McAgNP, the solution becomes slightly acidic. Before each measurement with UV–Vis spectrophotometry, suspension pH was adjusted. To better understand the results, the suspensions were numbered according to the plant material volume and $AgNO_3$ concentration. The results are summarized in Table 1, with their respective pH values before and after each adjustment. Figure 1 (a, b, c) shows the UV–Vis spectra before and after each pH adjustment.

The suspension-denominated McAg 2 was determined as the one with better characteristics and selected for the next steps of the study. This decision was made by reason of the characteristics of the SPR band:1) the higher intensity the band showing, the higher silver nanoparticles concentration in the suspension (better performance); 2) the narrower band, indicating more monodispersed suspensions, and 3) the shorter the wavelength pointing to the smaller particle sizes.

The next study was the analysis by reason of the gradual increase in pH. There was a significant increase in the intensity of the SPR band after the first adjustment (51%), which was followed by a less significant increase under pHs 9.1 (15%) and 10.7 (9%), where saturation occurs (Fig. S3 a and b in the ESM 1). It was observed that in suspensions with pH adjusted to values greater than 9.5, there was a reduction in pH, which stabilized around 7.5 (± 0.4).

Furthermore, a new analysis was performed. The suspension pH was set to 7.5 immediately after the addition of $AgNO_3$ to the extract. The promoted effects were observed by UV–Vis analysis in function of the reaction time (Figure S3 c and d in ESM 1). The reaction starts as soon as the pH is adjusted. Its pH rises to 21% after 30 min, where it stabilizes and presents a small improvement after 24hs (8%) and then remains stable.

DLS analyses which are presented in Table 2 indicate that the McAg 2 suspension (pH 7.5) has high monodispersity. However, it counts on some agglomerates. Zeta potential values close to − 30 mV indicate good stability and negative surface charge, leading to electrostatic repulsion of the particles.

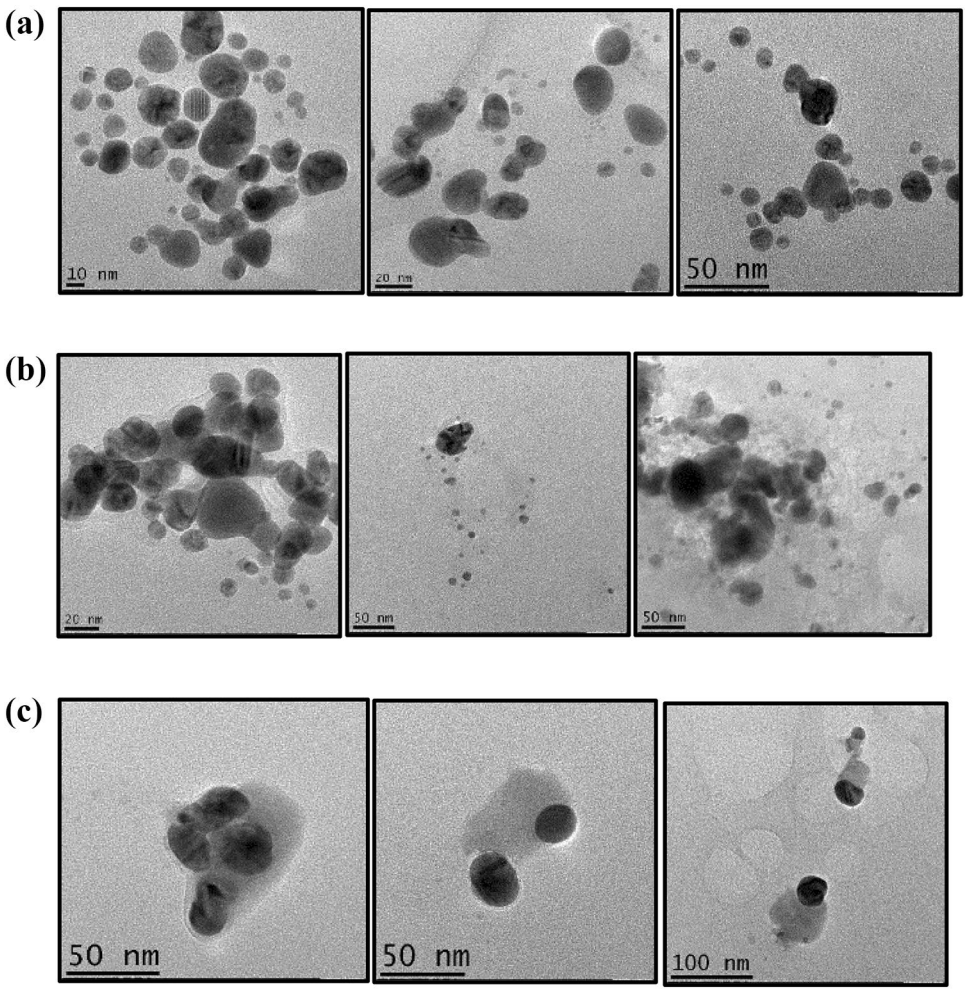

Fig. 7 TEM images of McAgNP in the presence of different concentrations of Hg^{2+} **a** 1 µg/mL; **b** 5 µg/mL; **c** 20 µg/mL

The stability of the McAgNP can be verified by UV–Vis spectra (Figure S4 in ESM 1), which presents only a discrete reduction in the absorbance intensity (8%) and a slight widening in the plasmonic band (20%) even 180 days after the preparation.

Images of TEM (Fig. 2) confirm the presence of spherical nanoparticles in the majority, with average diameters of 15 nm.

Since the reducing agent of the metal ions in this process is a natural material. It is susceptible to variations according to the climate and stage of development.

For the analysis of reproducibility, the spectra of three suspensions prepared during the rainy period and two during the dry climate period of McAg 2 pH ~ 7.5 were used. The leaves collected in the dry period were washed, chopped and frozen in Falcon tube for 5 months when the extract and a new sample were prepared. Similar characteristics were observed in all conditions (Fig S5 in ESM 1).

The UV–Vis absorption spectrum of the *M. coriacea* extract (Fig. 3 a) shows absorption bands in the UV region, indicating the presence of amino acids, carotenoids, and chlorophyll, which may be bound to McAgNP (Fig. 3a). The 218 nm band present in the extract and the McAgNP indicates the presence of tannins [31, 32].

The presence of alkaloids, tannins and other phenolic compounds in plants of the genus *Mimusops* and others of the *Sapotaceae* family has already been reported in previous studies [33–35]. Fluorescence spectra of the McAgNP and the *M. coriacea* extract without the addition of the metal were obtained to observe changes in the chlorophyll fluorescence present in the extract after the formation of the nanoparticles. In Fig. 3b, it is observed that the presence of AgNP induces suppression of chlorophyll fluorescence at 676 nm (samples excited at 430 nm).

The FTIR spectra of *M. coriacea* and McAgNP leaves extract are shown in Fig. 3c. The FTIR signal of the extract shows peaks around 3436, 2935, 1617, 1444 and 1049 cm^{-1}. The band at 3436 cm^{-1} occurred in function of the OH stretch. The band at 2935 cm^{-1} occurred as a result of the presence of aldehyde CH and was shifted to a lower frequency (2928 cm^{-1}) in McAgNP. The 1617 cm^{-1} band in

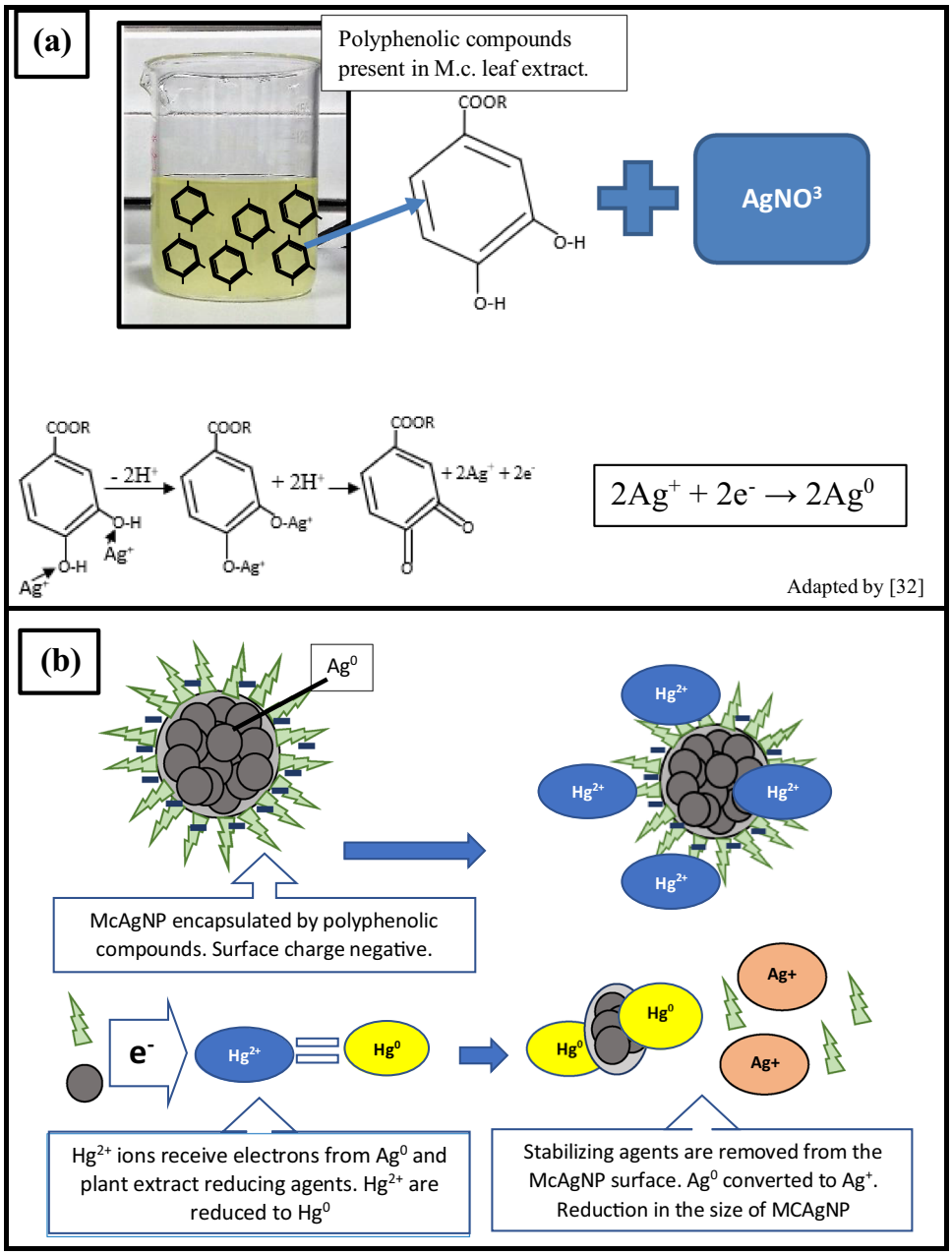

Fig. 8 Schematic representation of: **a** Ag^{+} reduction mechanism by polyphenolic compounds; **b** Hg^{2+} detection mechanism

M. coriacea leaf extract attributed to the presence of amide I vibrations was shifted to 1627 cm^{-1} in McAgNP probably as a consequence of the presence of proteins that possibly bound to the silver nanoparticles through the amine groups. The 1049 cm^{-1} band as a result of C–O–C stretching could be attributed to Ag^{+} reduction since the band was shifted to 1040 cm^{-1} in McAgNPs [34].

3.1 Analysis of sensitivity and selectivity to Hg^{2+}

As shown in Fig. 4, there is a significant reduction in the absorbance intensity of McAgNP in the presence of Hg^{2+} ions. The same behavior is not observed in the presence of other ions at the same concentrations, which confirms the selectivity of the method.

In Fig. 5, the UV–Vis spectra of McAgNP in the presence of the Hg^{2+} solutions at concentrations between 50 and 500 ng/mL are presented. It was observed that the changes in the McAgNP plasmonic band were proportional and linear to the increase in concentration. These changes can be observed in three parameters: absorbance intensity, λmax. position and band area between 320 and 600 nm.

Independent calibration curves were created for each of the altered parameters. When considering the reduction in the absorbance intensity and the band area between 320 and 600 nm, the LOD was 7.9 and 6.5 ng/mL, respectively, while

when considering the displacement of λmax, the LOD was 34.7 ng/mL. The mean reduction in absorption intensity and bandwidth was 7.5% (± 1.3) at each increase in Hg^{2+} concentration in the solution, while the blueshift was 1%, justifying the smaller LOD and LOQ when considering the first two parameters. Figure 6a, b, c presents the calibration curves created considering each parameter, with their respective LOD and LOQ.

The stability of the reaction was measured through UV–Vis spectrophotometry at 1-min intervals for 30 min, from a blank sample (McAgNP 1 mL + 5 mL high-purity water), and a prepared sample of McAgNP + Hg^{2+} at a concentration of 200 ng/mL.

Although there are changes in the parameters of the absorption band over time, this does not compromise the reliability of the method, because after 10 min of reaction, which is the time indicated by previous studies for the amalgamation, the variation does not exceed 7% in the bandwidth and absorbance intensity (Figure S6 a and b in ESM 1). In addition, no changes in the position of λmax were observed (Figure S6 c in ESM 1).

TEM images of the McAgNP shown in Fig. 7 were obtained after 30 min of reaction with Hg^{2+}. It is observed that the increase in the concentration of Hg^{2+} in the solution initially leads to the agglomeration of the McAgNP and in high concentrations, the number of particles is reduced, besides presenting a dark membrane species adhered to its surface, which possibly is the Hg^{2+} present in the solution.

As the McAgNPs were not diluted for this analysis, higher concentrations of Hg were used: 1 µg/mL (Fig. 7a), 5 µg/mL (Fig. 7b) and 20 µg/mL (Fig. 7c).

4 Discussion

Regarding the McAgNP synthesis, a significant increase in the absorbance intensity of the McAgNP was observed after pH adjustment. In addition, there is a small blue shift of λmax and the band becomes narrowing. A small difference has been observed between suspensions at neutral and basic pH. However, 24 h after adjustment there was a pH reduction in the adjusted suspensions to pH ≥ 9.5. This happened probably because of the release of H^+ ions in the medium during the extract oxidation process. The final pH of these solutions was 7.6 (± 0.3). This pH reduction was not observed in suspensions with pH adjusted between 6.5 and 7.5.

It was also possible to observe that extracts prepared with lower volume of plant material are favorable since the best results were obtained in this way. In contrast, the increase in the concentration of $AgNO_3$ in the solution leads to more concentrated colloidal suspensions. Previous studies about the AgNP synthesis from vegetable extracts have also reported that lower extract/silver ratios favor the reaction. In addition, the pH adjustment is indicated as a determinant factor for the reduction in metallic ions, so it is possible to control the nanoparticles size and stability of the nanoparticles. It has been reported that the synthesis of metallic nanoparticles mediated by plant extracts occurs at pH values between 2 and 14, depending on the species of the plant [33]. However, the neutral to slightly basic pH is considered ideal, as in these conditions there are a greater number of functional groups available, which facilitate the formation of a greater number of nanoparticles and avoiding agglomeration, which results in particles of smaller diameters. In addition, the neutral pH allows the application of nanomaterials. These applications occur mainly in the health and food areas. [33–38].

Thus, the results obtained indicate that the suspension named McAg 2 with adjustment of the medium for neutral to slightly basic is the ideal condition among those tested to obtain the nanoparticles by the proposed method, resulting in spherical particles with an average size of 15 nm.

The nanoparticles synthesis mechanism occurs by a redox reaction. Here, compounds present in the extract oxidize in the presence of the ionic metal, reducing them to the neutral atoms, followed by growth by agglomeration until its stabilization, which occurs by the encapsulation of the particles also by the compounds present in the extract.

A detailed characterization of the compounds present in the aqueous extract of *M. coriacea* leaves was not found in the literature. However, other species of the same genus have been characterized and the presence of tannins, alkaloids and other polyphenolic compounds can be attributed to the reduction in metal ions and encapsulation of the particles [34, 35].

We could experimentally observe the suppression of chlorophyll fluorescence after the formation of McAgNP. In addition, there are new bands at 467, 503, 587 and 706 nm, attributable to carotenoid pigments, which increase with the presence of nanoparticles. Xanthophyll, in this case, is the major carotenoid that exhibits an intramolecular charge-transfer state [38]. The results indicate that triplet states of chlorophyll were effectively suppressed by an energy transfer process to the carotenoids [38].

The action of tannins and other polyphenolic compounds (one or more hydroxyls attached to an aromatic ring) present in aqueous extracts is responsible for the reduction in metallic ions and the coating of the nanoparticles avoiding their agglomeration [31, 32, 36].

In this model of reaction, it is proposed that the reduction occurs by the hydroxyl groups present in the benzene ring. The process begins with the oxidation of the tannin in the presence of Ag^+ ions forming an intermediate complex. Ag^+ ions are then reduced to Ag^0, which collide to form agglomerates. Stabilization of nanoparticle growth possibly occurs

by encapsulation by the polyphenolic compound. Figure 8a schematically represents the proposed mechanism [32].

The McAgNP demonstrated excellent potential for the detection of Hg^{2+} ions in aqueous solution by the proposed method. The detection limit was 6.5 ng/mL (~ 32.5 nM) determined from the analytical curve construction as a function of changes in the plasmonic bands. Although some authors have reported the detection of Hg through changes in the plasmatic bands of NPs biosynthesized they generally depend on the functionalization of the AgNP through the addition of other molecules or obtain higher LOD than reported in the present study [9, 29].

The detection mechanism consists of the effects of a redox reaction between the Hg^{2+} ions and the zero-valent silver as a result of the greater reduction potential of Hg^{2+} in relation to Ag^{+} (0.80 V to $Ag^{+} \rightarrow Ag^{0}$, and 0.85 V–$Hg^{2+} \rightarrow Hg^{0}$). Phenolic compounds and their derivatives present in the leaves of *Mimusops* species have multifunctional groups such as hydroxyls and carboxylates that interact with metals and facilitate the bonding of mercury with the silver nanoparticle. In addition, the McAgNP encapsulated by these phenolic binders has a negative surface charge, capable of attracting the Hg^{2+} ions in the solution to its surface.

The compounds present in the extracts also act as reducing agents, since they reduce Ag^{+} to Ag^{0} in the synthesis process and reduce the Hg^{2+} to Hg^{0} ions in this case. These redox reactions lead to the removal of the stabilizing agent from the surface of the nanoparticles, which facilitates the Hg ions interaction with the Ag ones, which oxidizes to Ag^{+}. This process reduces the size of the particles justifying and blueshift of the plasmon band. When converting Ag^{0} to Ag^{+}, the concentration of the colloidal solution decreases, reducing the absorbance intensity and making the solution colorless when in high concentrations of Hg^{2+} indicating that the Ag^{0} atoms available in colloidal suspensions were oxidized. Figure 8b schematically demonstrates this mechanism.

5 Conclusions

The synthesis of AgNP using $AgNO_3$ as a metallic precursor and the *M. coriacea* aqueous extract obtained with the infusion of fresh leaves was possible. In the present study, we were able to eliminate the xenon lamp irradiation step, which is necessary in the previously reported procedure and makes the process faster and low cost. The phytochemicals present in the plant extract were the only ones responsible for the reduction in the metal ion through a static process, at room temperature and neutral pH without the need for centrifugation or additional steps as generally reported in similar studies. The McAgNP was monitored for 180 days, and we concluded that it remained stable during this period of time without the need to add other molecules: the components of the plant extract effective in encapsulation and maintaining stability. McAgNp showed excellent sensitivity and selectivity in the detection of Hg^{2+} in aqueous solution, with LOD of 6.5 ng/mL (32.5 nM), without the need for functionalization of AgNPs or the addition of other molecules. This detection limit is compatible with analysis of environmental samples such as fish, soil and effluent discharge. In addition to the application presented in this study, McAgNP has potential for application in several areas, in view of its excellent stability in neutral pH and sustainable synthesis process.

Supplementary information The online version contains supplementary material available at https://doi.org/10.1007/s00339-021-04391-2.

Acknowledgements The authors would like to thank CAPES for financial support and Multiuser Facilities Central at UFABC for the experimental support and São Paulo Research Foundation (FAPESP) for Grant #2017/23686-6.

Funding This research was funded by Coordenação de Aperfeiçoamento de Pessoal de Nível Superior – Brasil (CAPES) and Grant #2017/23686–6 of São Paulo Research Foundation (FAPESP).

Data availability Contact the authors for information on data availability.

Compliance with ethical standards

Conflict of interest There are no conflicts to declare.

References

1. UNEP (2019) Minamata Convention on Mercury. http://www.mercuryconvention.org/Convention/Text/tabid/3426/language/en-US/Default.aspx. Accessed 10 August 2020
2. BRASIL (2013) Diagnóstico Preliminar sobre o Mercúrio no Brasil. Ministério do Meio Ambiente
3. Farias L.A (2006) Avaliação do Conteúdo de Mercúrio, Metilmercúrio e Outros Elementos de Interesse em Peixes e em Amostras de Cabelos e Dietas de Pré-Escolares da Região Amazônica. Thesis, Universidade Federal de São Paulo
4. WAD J,(2010) Especiação, Quantificação, Distribuição e Transporte de Mercúrio em Solos Contaminados do Município de Descoberto, Belo Horizonte. Dissertation, Universidade Federal de Minas Gerais
5. F. Chai, C. Wang, T. Wang, Z. Ma, Z. Su, L-cysteine functionalized gold nanoparticles for the colorimetric detection of Hg^{2+} induced by ultraviolet light. Nanotechnology **21**(2), 025501 (2009). https://doi.org/10.1088/0957-4484/21/2/025501
6. J. Duan, H. Yin, R. Wei, W. Wang, Facile colorimetric detection of Hg^{2+} based on anti-aggregation of silver nanoparticles. Biosens. Bioelectron. **57**, 139–142 (2014). https://doi.org/10.1016/j.bios.2014.02.007
7. L. Li, B. Li, Y. Qi, Y. Jin, Label-free aptamer-based colorimetric detection of mercury ions in aqueous media using unmodified gold

nanoparticles as colorimetric probe. Anal. Bioanal. Chem. **393**(8), 2051–2057 (2009). https://doi.org/10.1007/s00216-009-2640-0
8. G. Sener, L. Uzun, A. Denizli, Lysine-promoted colorimetric response of gold nanoparticles: a simple assay for ultrasensitive mercury(II) detection. Anal. Chem. **86**(1), 514–520 (2014). https://doi.org/10.1021/ac403447a
9. P. Sharma et al., Thiol terminated chitosan capped silver nanoparticles for sensitive and selective detection of mercury (II) ions in water. Sens. Actuators B: Chem. **268**, 310–318 (2018). https://doi.org/10.1016/j.snb.2018.04.121
10. Albernaz VL (2014) Síntese verde de nanopartículas de prata com extrato aquoso de folhas de *Brosimum gaudichaudii*, caracterização fisicoquímica, morfológica e suas aplicações no desenvolvimento de um nanobiossensor eletroquímico. Dissertation, Universidade de Brasilia
11. S. Iravani, Green synthesis of metal nanoparticles using plants. Green Chem. **13**(20), 2638 (2011). https://doi.org/10.1039/C1GC15386B
12. A. Mishra et al., Microbial synthesis of gold nanoparticles using the fungus *Penicillium brevicompactum* and their cytotoxic effects against mouse mayo blast cancer C2C12 cells. Appl. Microbiol. Biotechnol. **92**(3), 617–630 (2011). https://doi.org/10.1007/s00253-011-3556-0
13. V.K. Sharma, R.A. Yngard, Y. Lin, Silver nanoparticles: green synthesis and their antimicrobial activities. Adv. Coll. Interface. Sci. **145**, 83–96 (2009). https://doi.org/10.1016/j.cis.2008.09.002
14. H. Itoh, K. Naka, Y. Chujo, Synthesis of gold nanoparticles modified with ionic liquid based on the imidazolium cation. J. Am. Chem. Soc. **126**(10), 3026–3027 (2004). https://doi.org/10.1021/ja039895g
15. P. Singh, K. Kumari, A. Katyal, R. Kalra, R. Chandra, Synthesis and characterization of silver and gold nanoparticles in ionic liquid. Spectrochim. Acta Part A Mol. Biomol. Spectrosc. **73**(1), 218–220 (2009). https://doi.org/10.1016/j.saa.2009.02.007
16. R. Lu, D. Yang, D. Cui, Z. Wang, L. Guo, Egg white-mediated green synthesis of silver nanoparticles with excellent biocompatibility and enhanced radiation effects on cancer cells. Int. J. Nanomed. **7**, 2101–2107 (2012). https://doi.org/10.2147/IJN.S29762
17. R.A. De Matos, L.C. Courrol, Saliva and light as templates for the green synthesis of silver nanoparticles. Coll. Surf.A Physicochem. Eng. Asp. **441**, 539–543 (2014). https://doi.org/10.1016/j.colsurfa.2013.10.009
18. J.L. Gardea-Torresdey, E. Gomez, J.R. Peralta-Videa, J.G. Parsons, H. Troiani, M. Jose-Yacaman, Alfalfa sprouts: a natural source for the synthesis of silver nanoparticles. Langmuir **19**(4), 1357–1361 (2003). https://doi.org/10.1021/la020835i
19. A.K. Mittal, Y. Chisti, U.C. Banerjee, Synthesis of metallic nanoparticles using plant extracts. Biotechnol. Adv. **31**, 346–356 (2013). https://doi.org/10.1016/j.biotechadv.2013.01.003
20. P. Rauwel, S. Kuunal, S. Ferdov, E. Rauwel, A review on the green synthesis of silver nanoparticles and their morphologies studied via TEM. Adv. Mater. Sci. Eng. (2015). https://doi.org/10.1155/2015/682749
21. J. Park, S.-H. Cha, S. Cho, Y. Park, Green synthesis of gold and silver nanoparticles using gallic acid: catalytic activity and conversion yield toward the 4-nitrophenol reduction reaction. J. Nanopart. Res. **18**(6), 166 (2016). https://doi.org/10.1007/s11051-016-3466-2
22. C.R.B. Lopes, L.C. Courrol, Green synthesis of silver nanoparticles with extract of *Mimusops coriacea* and light. J. Lumin. **199**, 183–187 (2018). https://doi.org/10.1016/j.jlumin.2018.03.030
23. D. Wang, Q. Gai, R. Huang, X. Zheng, Label-free electrochemiluminescence assay for aqueous Hg^{2+} through oligonucleotide mediated assembly of gold nanoparticles. Biosens. Bioelectron. **98**, 134–139 (2017). https://doi.org/10.1016/j.bios.2017.06.054
24. Y. Liu et al., Turn-on fluoresence sensor for Hg^{2+} in food based on fret between aptamers-functionalized upconversion nanoparticles and gold nanoparticles. J. Agric. Food Chem. **66**(24), 6188–6195 (2018). https://doi.org/10.1021/acs.jafc.8b00546
25. S. Jia, C. Bian, J. Sun, J. Tong, X. Shanhong, A wavelength-modulated localized surface plasmon resonance (LSPR) optical fiber sensor for sensitive detection of mercury(II) ion by gold nanoparticles-DNA conjugates. Biosens Bioelectron **114**, 15–21 (2018). https://doi.org/10.1016/j.bios.2018.05.004
26. A.N. Vijayan, L. Zhiming, Z. Haohan, P. Zhang, Nicking enzyme-assisted signal-amplifiable Hg^{2+} detection using upconversion nanoparticles. Anal. Chim. Acta **1072**, 75–80 (2019). https://doi.org/10.1016/j.aca.2019.05.001
27. C.O. Amorim et al., Ultra sensitive quantification of Hg^{2+} sorption by functionalized nanoparticles using radioactive tracker spectroscopy. Microchem. J. **138**, 418–423 (2018). https://doi.org/10.1016/j.microc.2018.01.039
28. P. Preposito et al., Bifunctionalized silver nanoparticles as hg^{2+} plasmonic sensor in water: synthesis, characterizations, and ecosafety. Nanomaterials **9**(10), 1353 (2019). https://doi.org/10.3390/nano9101353
29. S. Ghosh, S. Maji, A. Mondal, Study of selective sensing of Hg^{2+} ions by green synthesized silver nanoparticles suppressing the effect of Fe^{3+} ions. Colloids Surf., A **555**, 324–331 (2018). https://doi.org/10.1016/j.colsurfa.2018.07.012
30. L. Currie, Detection and quantification limits: origins and historical overview. Anal. Chim. Acta **391**, 127–134 (1999). https://doi.org/10.1016/S0003-2670(99)00105-1
31. E. Bulut, Rapid, facile synthesis of silver nanostructure using hydrolyzable tannin. Ind. Eng. Chem. Res. (2009). https://doi.org/10.1021/ie801779f
32. K.J. Rao, S. Paria, Green synthesis of silver nanoparticles from aqueous *Aegle marmelos* leaf extract. Mater. Res. Bull. **48**(2), 628–634 (2013). https://doi.org/10.1016/j.materresbull.2012.11.035
33. Z. Mashwani, T. Khan, M.A. Khan, A. Nadhman, Synthesis in plants and plant extracts of silver nanoparticles with potent antimicrobial properties: current status and future prospects. Appl. Microbiol. Biotechnol. **99**, 9923–9934 (2015). https://doi.org/10.1007/s00253-015-6987-1
34. P. Prakash, P. Gnanaprakasam, R. Emmanuel, S. Arokiyaraj, M. Saravanan, Green synthesis of silver nanoparticles from leaf extract of *Mimusops elengi, Linn*. for enhanced antibacterial activity against multi drug resistant clinical isolates. Coll. Surf. B: Biointerf. **108**, 255–259 (2013). https://doi.org/10.1016/j.colsurfb.2013.03.017
35. S. Satish, M.P. Raghavendra, D.C. Mohana, K.A. Raveesha, Antifungal activity of a known medicinal plant Mimusops elengi L against grain moulds. J Agric Technol **4**(1), 151–165 (2008)
36. S. Rajeshkumar, L.V. Bharath, Mechanism of plant-mediated synthesis of silver nanoparticles – a review on biomolecules involved, characterization and antibacterial activity. Chem. Biol. Interact. **273**, 219–227 (2017). https://doi.org/10.1016/j.cbi.2017.06.019
37. R. Veerasamy et al., Biosynthesis of silver nanoparticles using mangosteen leaf extract and evaluation of their antimicrobial activities. J. Saudi Chem. Soc. **15**(2), 113–120 (2011). https://doi.org/10.1016/j.jscs.2010.06.004
38. P. Khoroshyy, D. Bína, Z. Gardian, R. Litvín, J. Alster, J. Pšenčík, Quenching of chlorophyll triplet states by carotenoids in algal

light-harvesting complexes related to fucoxanthin-chlorophyll protein. Photosynth. Res. **135**(1–3), 213–225 (2018). https://doi.org/10.1007/s11120-017-0416-5

Publisher's Note Springer Nature remains neutral with regard to jurisdictional claims in published maps and institutional affiliations.